Ion-Exchange Adsorption of Calcium Ions from Water and Geothermal Water with Modified Zeolite A

Junchao Song
School of Chemical Engineering and Technology, Tianjin University, Tianjin 300072, China

Mingyan Liu
School of Chemical Engineering and Technology, Tianjin University, Tianjin 300072, China

State Key Laboratory of Chemical Engineering (Tianjin University), Tianjin 300072, China

Yang Zhang
School of Chemical Engineering and Technology, Tianjin University, Tianjin 300072, China

DOI 10.1002/aic.14671
Published online November 21, 2014 in Wiley Online Library (wileyonlinelibrary.com)

The modified zeolite A was prepared by a two-step crystallization method to remove scale-forming cations from water and geothermal water. The adsorption kinetics, mechanism and thermodynamics were studied. The calcium ion adsorption capacity of the modified zeolite A was 129.3 mg/g (1 mg/g = 10^{-3} kg/kg) at 298 K. The adsorption rate was fitted well with pseudo-second-order rate model. The adsorption process was controlled by film diffusion at the calcium ion concentration less than 250 mg/L (1 mg/L = 10^{-3} kg/m^3), and it was controlled by intraparticle diffusion at the concentration larger than 250 mg/L. The calculated mass-transfer coefficient ranged from 2.23 × 10^{-5} to 2.80 × 10^{-4}cm/s (1 cm/s = 10^{-2}m/s). Dubinin–Astakhov isotherm model could appropriately describe the adsorption thermodynamic properties when combined with Langmuir model. The adsorption process included not only ion exchange but also complexation between calcium and hydroxyl ions. The adsorption was spontaneous and endothermal. The high adsorption capacity indicates that the modified zeolite A is a suitable adsorption material for scale removal from aqueous solution.
 AIChE J, 61: 640–654, 2015
Keywords: calcium ion, ion-exchange adsorption, modified zeolite A, adsorption mechanism, calcium removal efficiency

Introduction

Scaling in heat exchanger and pipeline is the key challenge in the process of geothermal energy utilization, which exists for a long time and demands prompt solution.[1] Several methods such as chemical inhibitor,[2] physical field,[3] surface modification[4] have been utilized to avoid scale formation in easy-to-scaling water. However, chemical inhibitor is uneconomical and may be an additional contamination. The other methods cannot solve scaling problem thoroughly because scale depositing on the surface is inevitable in practice.

The major ions in geothermal water include Cl^-, SO_4^{2-}, HCO_3^-, Na^+, K^+, Ca^{2+}, and Mg^{2+}.[5] Among them, the calcium ions can easily form carbonate and sulphate scales, which are the main forms of scales existing in the low and middle temperature geothermal fields. Supposing that the scale-forming cations are removed from geothermal water before entering heat exchanger, the scaling problem will be solved thoroughly. Hitherto, few researches were reported on the descaling through the removal of scale-forming ions in geothermal water.[6,7] However, quite a few studies about the removal of calcium, magnesium, and other ions from seawater and brine can lend us some added insight into the scale-forming cations removal from geothermal water. The methods of specific ions removal from solutions include precipitation, reverse osmosis, nanofiltration, adsorption, ion exchange, and so on. Among them, adsorption and ion exchange are probably the most effective and renewable methods, especially for the low concentration of adsorbate.[8–11]

In the research of the calcium and magnesium ions removals from brine and seawater, zeolite A and its analogues were usually used as adsorbents.[9,10,12–15] Herrmann et al.[10] facilitated the calcium removal with zeolite A as a pretreatment to prevent calcium sulfate scaling at the membranes. Whereas, the performance of zeolite A was not very favorable compared with the standard resins due to the cost and the electroselectivity caused by high concentration of salinity. In the process of water softening, Coker et al.[13] prepared the quasi-crystalline aluminosilicate zeolite precursors and investigated the kinetics of binary ion exchange of calcium and magnesium ions for sodium ions in the quasi-crystalline and crystalline zeolite A. It was found that the diffusion rates of calcium and magnesium ions in the crystalline zeolite A were relatively faster than that in the quasi-crystalline precursors. Yet, the relationship between the ion-exchange rate and the structural characteristics of the quasi-crystalline precursor was not clarified. Muraviev et al.[14] evaluated the influences of ion-exchange adsorbent properties on the

Correspondence concerning this article should be addressed to M.Y. Liu at myliu@tju.edu.cn.

efficiency of seawater decalcification process by simultaneous use of the electroselectivity reversal and ion-exchange isothermal supersaturation effects under continuous and closed-cycle operation mode. The results showed that the A-type zeolite modified by the sequential treatment with dilute magnesium-containing solution and concentrated sodium salt solution had higher efficiency than other ion-exchange resins. Recently, Qin et al.[9,12] carried out the research of calcium removal from simulated seawater with A-type zeolite, and investigated the effect of pH value on adsorption capacity by the competitive adsorption models. The adsorption capacity was 105 mg/g at the optimum condition.

In addition, the adsorption kinetics, thermodynamics, and the effects of operating conditions on the adsorption efficiencies of several kinds of ions with zeolite A were investigated in previous studies. El-Nagar et al.[16] and El-Kamash[17] investigated the removal performances of strontium and cesium from aqueous solution using zeolite A under batch and fixed bed operation systems, respectively. El-Kamash et al.[18] also studied the adsorption behaviors of zinc and cadmium ions from aqueous solution using zeolite A by batch operation. The adsorption thermodynamics and kinetics were discussed based on empirical models, as well as the ion diffusion behavior. It was pointed out that some heterogeneity in the surface and pores of zeolite would play a role in the adsorption of metal ions. However, the heterogeneity characteristics of zeolite and the relationship between the heterogeneity and the adsorption performance were not explored.

Previous work has extensively explored the performances of the calcium and magnesium ions removals from brine and seawater by ion exchange and adsorption methods. However, several fundamental issues including the diffusion mechanism, the nature of adsorption and the effect of the physicochemical property of adsorbent on the adsorption kinetics and equilibrium were not clarified in detail. Besides, it is well known that temperature is a critical factor determining the rate of ion-exchange adsorption. In the system of geothermal energy utilization, the temperature of geothermal water is generally higher than 303 K. Hence, it has special significance to investigate the influence of temperature on the adsorption kinetics and adsorption equilibrium. In addition, the calcium and sodium chloride concentrations in geothermal water are generally lower than that in brine and sea water. Therefore, it is expected that the calcium removal efficiency with zeolite in the geothermal water will be higher than that in the brine and seawater. However, there are few reports on the removal performances of calcium and magnesium ions considering the characteristics of geothermal water, and less exploration on the diffusion mechanism and the adsorption kinetics of calcium ions with zeolite from a quantitative point of view. Moreover, to ensure the utilization efficiency of geothermal energy, it is important to improve the adsorption rate of calcium ions as quickly as possible to minimize the losses of heat and mechanical energies. One feasible way is to change the surface morphology and the pore structure of absorbent to minimize the particle diffusion resistance, eventually to increase the calcium removal rate from aqueous solution.

Therefore, the modified zeolite A was prepared by a two-step crystallization method in this work. The performances of calcium ion removal from water and geothermal water with the modified zeolite A were investigated, especially for the adsorption kinetics and thermodynamics by means of several kinetic, isotherm models. The diffusion mechanism of the adsorption process was also discussed.

Experimental

Materials

The reagents used in this work were of AR grade chemicals, except of $NaAlO_2$ which was of CP grade. The $CaCl_2$ solution was prepared by dissolving $CaCl_2{\cdot}2H_2O$ in deionized water. The geothermal water was taken from a geothermal well in Tianjin, China.

Preparation of modified zeolite A

The 2.0 mol/L (1 mol/L = 10^3 mol/m^3) NaOH solution with the volume of 98.7 mL (1 mL = 10^{-6} m^3) was prepared and divided into two aliquots with the volume ratio of 4:6. The smaller aliquot was used to dissolve $Na_2SiO_3{\cdot}9H_2O$, and the larger aliquot was used to dissolve $NaAlO_2$. Afterward, the two parts of the solutions were mixed together with vigorous agitation for 5 min at room temperature. The resulting solution was transferred into the PTFE bottle and sealed and crystallized for 1 h (1 h = 3600 s) at 333 K. After that, the 0.667 mol/L cetyltrimethylammonium bromide (CTAB) solution with the volume of 30 mL was dropped into the solution, and the stirring was continued at 333 K for 1 h. The mole composition of the gel was $4Na_2O{:}Al_2O_3{:}SiO_2{:}0.4$CTAB$:152H_2O$. After that, 50 wt % sulfuric acid was used to adjust the pH of the sol to 12.0. The resulting sol was sealed and crystallized at 403 K for 24 h. The solid product was received by filtration and drying at 373 K overnight. The as-synthesized sample was then calcined under air atmosphere at 823 K for 5 h. The traditional zeolite A was synthesized according to the work of Thompson and Huber.[19]

Characterization

The powder x-ray diffraction (XRD) patterns of the samples were recorded with the Bruker D8 Focus diffractometer using Cu K_α radiation (40 kV, 40 mA). Scanning electron micrographs (SEM) were recorded using the Hitachi S4800 microscope. The samples were adhered to aluminium stubs by a thin layer of conducting carbon paste and sputter-coated with gold. Zeolite of 2 mg (1 mg = 10^{-6} kg) was suspended in 100 mL deionized water and subjected to ultrasonic vibration for 5 min to ensure a uniform distribution. Particle-size distribution and mean particle diameter were measured using a light scattering technique by a Malvern Instrument (Mastersizer S Long Bed).

Kinetic measurement

Batch adsorption experiments were performed at 298 K to determine the adsorption kinetics. $CaCl_2$ aqueous solution of 200 mL with the calcium ion concentration of 100 mg/L was agitated on a constant temperature magnetic stirrer with the magnetic rotor at the stirring speed of 600 r/min (rotations per minute). When the desired temperature reached, 0.2 g (1 g = 10^{-3} kg) of the adsorbent was added into the solution. At a predetermined interval of time, the calcium ion concentration was monitored on-line by an ion-activity meter[20–22] (Shanghai INESA Instrument, Lei-ci PXSJ-226). To verify the reliability of measurement results, 10 bottles $CaCl_2$ solutions with calcium ion concentrations between 10 and 500 mg/L were prepared before the experiments. The calcium ion concentrations were measured by both ion-activity meter method and EDTA titration method. Afterward, the ratio of the calcium ion concentration measured by ion-activity meter to the value achieved by EDTA method was calculated as an objective function to estimate the reliability of the experimental data. The confidence intervals of the 95% confidence level for the ratios at the temperature of

298 K, 303 K, 313 K were (0.9557, 0.9922), (0.9590, 1.0388), (0.9435, 0.9891), respectively.

In addition, the relative standard deviation (RSD) of adsorption amount for every measurement point was calculated according to the equation as follows

$$\mathrm{RSD}=\left\{\sqrt{\frac{\sum_{i=1}^{n}(q_i-\bar{q})^2}{n-1}}/\bar{q}\right\}\times 100\% \quad (1)$$

where q_i (mg/g) is the adsorption amount of the No. i experiment for any measurement point, $\bar{q}$ (mg/g) is the mean adsorption amount of the n times experiments for every measurement point, n is the times of the same experiment finished. The smaller the value of RSD, the better the repeatability and accuracy.

The amount of calcium ions adsorbed onto the adsorbent at a time t, q_t (mg/g), was calculated by the following equation

$$q_t=\frac{(C_0-C_t)\cdot V}{m} \quad (2)$$

where C_0 (mg/L) and C_t (mg/L) are the initial concentration and the concentration at any interval time of calcium ions in solution, respectively. V (L, 1 L = 10^{-3} m^3) is the volume of the solution and m (g) is the amount of absorbent added into the solution.

Adsorption equilibrium experiment

The 100 mL $CaCl_2$ solution with given calcium ion concentration (80–800 mg/L) was stirred with 0.1 g of adsorbent in a 250 mL conical flask at the temperature from 298 to 333 K. The pH was measured by a pH meter (Shanghai INESA Instrument, Lei-ci PHB-4), and initial pH was 5.5–6.0. When the adsorption equilibrium reached (1 h), the calcium ion concentration was detected by the EDTA titration method. The experiment was carried out in triplicate for each point.

A series of adsorption experiments in the geothermal water with calcium ion concentration from 17.5 to 1002.3 mg/L were carried out. The geothermal water with calcium ion concentration more than 102.6 mg/L was obtained by adding $CaCl_2{\cdot}2H_2O$ into the primary geothermal water to increase the corresponding calcium ion concentration in geothermal water. The conditions of the adsorption equilibrium experiments for the geothermal water were the same as that for the $CaCl_2$ solution except of the adsorption temperature of 298 K.

Regeneration of modified zeolite A

The 2–20 wt % NaCl solutions were used to regenerate the zeolite saturated by calcium ions.[14,23] Zeolite of 2.0 g saturated by $CaCl_2$ solution was used in the regeneration experiment. NaCl solution of 200 mL was divided equally into three aliquots and successively added into the beaker loaded with the saturated zeolite. So the dosage of the NaCl solution was 100 mL/g zeolite. The volume of the regeneration solution was only one-tenth of the volume of the $CaCl_2$ solution in the adsorption equilibrium experiment or the adsorption kinetics experiment. One reason was that it was difficult to refilter and collect the zeolite from the NaCl solution after regeneration for a little amount of zeolite (0.1 or 0.2 g). Another was that it was cost-saving and high-efficiency for regeneration of the saturated zeolite due to the use of the less amount and high concentration of NaCl solution. Batch regeneration experiment was performed at 298 K for 1 h, then the zeolite was filtered from the suspension solution. After that, the experiment proceeded to desorb the calcium ions from the zeolite until finishing the desorption for three times. The regenerated zeolite was washed with deionized water and dried at 393 K for 12 h.

Theoretical Models

Kinetic models

Pseudo-First-Order Rate Model. The Lagergren rate equation is the first rate equation for the adsorption of liquid-solid system based on solid capacity,[24] which can be presented in a linear form

$$\log(q_e-q_t)=\log q_e-\frac{k_1}{2.303}t \quad (3)$$

where q_e is the amount of calcium ions adsorbed on the zeolite at equilibrium (mg/g), q_t is the amount of calcium ions adsorbed on the zeolite at time t (mg/g), k_1 is the pseudo-first rate constant (min^{-1}, 1 min^{-1} = 1/60 s^{-1}).

Pseudo-Second-Order Rate Model. The pseudo-second-order rate equation is based on the assumption that the sorption capacity is proportional to the number of active sites occupied on the sorbent. The equation is with the peat-copper reaction as the most typical representative of the pseudo-second-order sorption mechanism.[25,26] Its linear form can be expressed as

$$\frac{t}{q_t}=\frac{1}{k_2q_e^2}+\frac{1}{q_e}t \quad (4)$$

where k_2 is the pseudo-second-order rate constant (g mg^{-1} min^{-1}, 1 g mg^{-1} min^{-1} = 50/3 kg kg^{-1} s^{-1}).

Diffusion models

Effective Diffusion Coefficient Model. The process of ion-exchange adsorption is quite complex due to the diffusion, adsorption, ion exchange, and even reaction process involved. Generally, the step of ion exchange is very rapid and not the rate-determining step in the uptake of organic and inorganic compounds.[27,28] To clarify adsorption mechanism and identify the step governing the overall rate of the adsorption process: film diffusion or intraparticle diffusion, the Boyd[29] and Helfferich[30] model was used. Under the conditions that the particle diffusion was the sole rate-controlling step, the following expression was suggested

$$F(t)=1-\frac{6}{\pi^2}\sum_{n=1}^{\infty}\frac{1}{n^2}\exp\left(-\frac{D_i\pi^2n^2t}{r_0^2}\right) \quad (5)$$

or

$$F(t)=1-\frac{6}{\pi^2}\sum_{n=1}^{\infty}\frac{1}{n^2}\exp(-n^2Bt)\ \text{then},\ B=\frac{\pi^2D_i}{r_0^2} \quad (6)$$

where F is the fractional attainment of equilibrium at time t and defined as $F(t)=q_t/q_\infty$, q_t is the amount of adsorbate adsorbed at time t (mg/g), q_∞ is the maximum equilibrium amount adsorbed (mg/g). D_i is the effective diffusion coefficient of ions into adsorbent (m^2/s), r_0 is the radius of adsorbent particle (m), and n is an integer defining the infinite series solution.

If the process is governed by intraparticle diffusion, the value of B should be constant.[29] The values of Bt against the

experimental values of t can be plotted in a straight line passing through the origin point with the slope of B, provided that the diffusion coefficient D_i does not vary with F.[31] Otherwise, the process may be controlled by film diffusion. Furthermore, knowing the particle size r_0, an average value of D_i can be obtained. The suitable expressions of Bt transformed from the equation of intraparticle diffusion mechanism within two different ranges of F were used to obtain the values of Bt.[31] It is more accurate to obtain the values of Bt for a series of values of F by this means than by the method of looking up the values from the Reichenberg's table.[27,32]

For $F = 0$–0.85

$$F=\frac{6}{\pi^{3/2}}\sqrt{Bt}-\frac{3}{\pi^2}(Bt) \tag{7}$$

It is transformed to

$$Bt=2\pi-\frac{\pi^2 F}{3}-2\pi\left(1-\frac{\pi F}{3}\right)^{1/2} \tag{8}$$

For $F = 0.85$–1

$$F=1-\frac{6}{\pi^2}e^{-Bt} \tag{9}$$

It is transformed to

$$Bt=-2.30258\log(1-F)-0.49770 \tag{10}$$

Surface Mass-Transfer Coefficient Model. The mass-transfer coefficient method proposed by McKay[33] was also used to further demonstrate mass transfer at the interfaces between the aqueous solution and the zeolite particles, for the initial stage of the ion-exchange adsorption process. The model can be expressed as

$$\ln\left(\frac{C_t}{C_0}-\frac{1}{1+mK}\right)=\ln\frac{mK}{1+mK}-\frac{1+mK}{mK}\beta_L S_s t \tag{11}$$

where C_t is the concentration of adsorbate at t (mg/L), C_0 is the initial concentration of adsorbate (mg/L), K is the Langmuir constant, which is corresponding to the product of adsorption capacity q_0 and energy parameter b in Langmuir equation (the calculated values of the parameter are described below), β_L is the surface mass-transfer coefficient (cm/s), m is the mass of adsorbent particles per unit volume of particle-free adsorbate solution (g/L, 1 g/L = 1 kg/m^3), and S_s is the outer surface of adsorbent particles per unit volume of particle-free slurry (cm^{-1}, 1 cm^{-1} = 10^2 m^{-1}), which can be obtained from m based on the assumption of smooth spherical particles and presented as

$$S_s=\frac{6m}{d_p\rho_p(1-\varepsilon_p)} \tag{12}$$

where d_p is the particle diameter (cm, 1 cm = 10^{-2} m) and ρ_p is the density of adsorbent particles (g/cm^3, 1 g/cm^3 = 10^3 kg/m^3) and ε_p is the porosity of adsorbent particles.

Adsorption isotherms

The adsorption equilibrium is usually described by isotherm equations, in which the parameters generally indicate the surface physicochemical property, the structure characteristics of adsorbent and the affinity between adsorbate and adsorbent.[34] To gain insight into the nature of the adsorption and the affinity of the adsorbent and adsorbate, several representative adsorption isotherm models including Langmuir, Dubinin–Radushkevich (D–R) and its general form Dubinin–Astakhov (D–A) isotherm equations were used to fit the isotherm experimental data.

Langmuir Isotherm. The Langmuir equation is probably the best known and most widely applied adsorption isotherm, which has been utilized to fit experimental data for a wide variety of liquid-solid phase adsorption systems.[17,35,36] It can be presented as follows

$$q_e=\frac{Q_0 b C_e}{1+bC_e}, \tag{13}$$

be linearized as

$$\frac{Ce}{q_e}=\frac{1}{Q_0 b}+\frac{1}{Q_0}C_e \tag{14}$$

where q_e is the amount of the calcium ions adsorbed on the zeolite at equilibrium (mg/g), C_e is the equilibrium concentration of the calcium ions in solution (mg/L), Q_0 is the maximum adsorption capacity (mg/g), b is the Langmuir equilibrium constant, which is related to the adsorption free energy.

D–R and D–A Isotherms. The D–R and D–A isotherms are both based on the Dubinin adsorption potential theory.[37] They will give an insight into the nature of the adsorption as well as the relationship between the adsorption free energy and the structure, surface physicochemical property of the adsorbent. The D–R equation can be written in linear form as follows

$$\ln q_e=\ln q_m-\beta\varepsilon^2 \tag{15}$$

with

$$\varepsilon=RT\ln\left(1+\frac{1}{Ce}\right) \tag{16}$$

where q_e is the amount of metal ions retained in the zeolite phase (mmol/g, 1 mmol/g = 1 mol/kg), q_m is the maximum amount of ions that can be adsorbed onto unit weight adsorbent (mmol/g), essentially q_m is the maximum adsorption capacity in pure zeolite,[38] β is the constant related to the sorption energy (mol^2/kJ^2, 1 mol^2/kJ^2 = 10^{-6} mol^2/J^2) and ε is the Polanyi potential, whose expression is analogous to that of the adsorption of gases and vapors onto microporous adsorbents based on the micropore volume filing theory.[39] R is the ideal gas constant (kJ mol^{-1} K^{-1}, 1 kJ mol^{-1} K^{-1} = 10^3 J mol^{-1} K^{-1}), and T is the absolute temperature (K). The mean energy of adsorption, denoted as E (kJ/mol, 1 kJ/mol = 10^3 J/mol), means that the free energy changes when one mole of ions are transferred from the infinity in the solution (the bulk of the solution) to the surface of the solid,[17] which can be calculated from the expression as below

$$E=\frac{1}{\sqrt{2\beta}} \tag{17}$$

In addition, the magnitude of E is useful for estimate the type of adsorption. If the value of $E < 8.0$ kJ/mol, the adsorption process may belong to physical adsorption; if the value of E is in the range of 8–16 kJ/mol, the adsorption is governed mainly by ion-exchange process.[28]

To clarify the effects of the pore structure and the surface physicochemical property of adsorbent on the adsorption free energy, the Dubinin–Astakhov model which possesses more universal significance was used to study the adsorption process. Its exponential form is given as

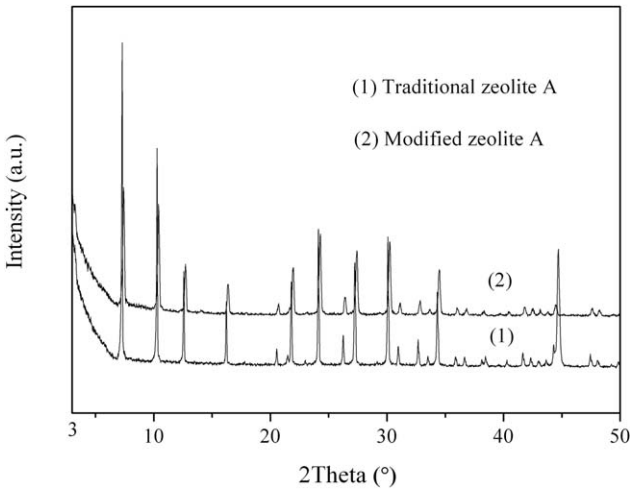

Figure 1. XRD patterns of zeolites from two different methods.

$$q_e = q_m \cdot \exp\left[-\left(\frac{RT\ln\left(1+\frac{1}{c_e}\right)}{\sqrt{2}\cdot E}\right)^n\right] \quad (18)$$

where n is the heterogeneity parameter, whose value depends on both the adsorbent and adsorbate properties, and the other parameters have the same meanings as described in the D–R model. Based on the experimental equilibrium data, if the adsorption capacity q_m is acquired, then the D–A equation can be forced to fit the experimental data to gain the values of heterogeneity parameter (n) and adsorption free energy (E).

Results and Discussion

Characterization of modified zeolite A

The x-ray powder diffraction patterns of the modified zeolite A and the traditional zeolite A are shown in Figure 1. The XRD patterns display that the crystalline phase of the modified zeolite is consistent with that of the traditional zeolite A,[40] indicating that the modified zeolite A may possess similar physicochemical properties of the traditional zeolite A. Besides, there is no mixed crystal phase coexisting in the modified zeolite A, and the crystallinity of the modified zeolite A is slightly lower compared with the traditional zeolite A. The graphs of SEM shown in Figure 2 demonstrate that the surface morphology of the modified zeolite A is different from that of the traditional zeolite A. The modified zeolite A has lots of lamellate and needle-like crystals instead of the main cubic crystals, which may lead to some difference of surface physicochemical property compared with the traditional zeolite A. Besides, the grain sizes of the modified zeolite A are mainly 2–4 μm (1 $\mu m = 10^{-6}$ m) in diameter. The particle-size distribution is presented in Figure 3. The mean particle diameter (D_{50}) was estimated to be 2.62 μm, and a 0.87% of particles smaller than 0.5 μm were obtained.

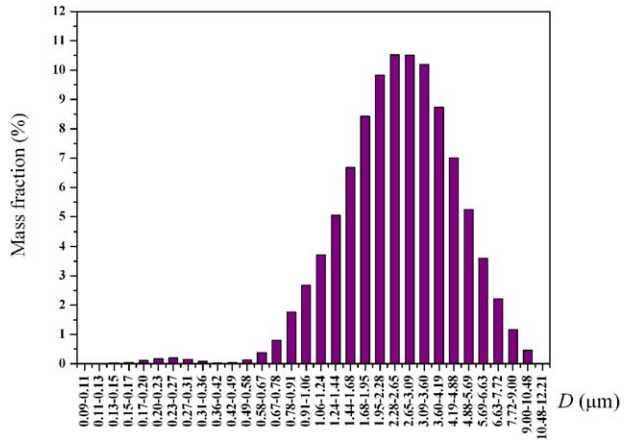

Figure 3. Particle-size distribution of modified zeolite A (1 $\mu m = 10^{-6}$ m).

[Color figure can be viewed in the online issue, which is available at wileyonlinelibrary.com.]

Performance of calcium ion removal

The initial calcium ion concentration of the solution, 100 mg/L, was corresponding to that of the geothermal water in the region of North China.[5] The calcium ion removal performances of both the traditional zeolite A and the modified zeolite A are presented in Figure 4. The calcium ion concentration declines sharply in the initial stage of 10 min. After that, the degree of decline obviously decreases due to the process approaching to adsorption equilibrium. The adsorption equilibrium basically achieved after 1 h. Meanwhile, the adsorption capacity and adsorption rate of the modified zeolite A were greater than that of the traditional zeolite A. The

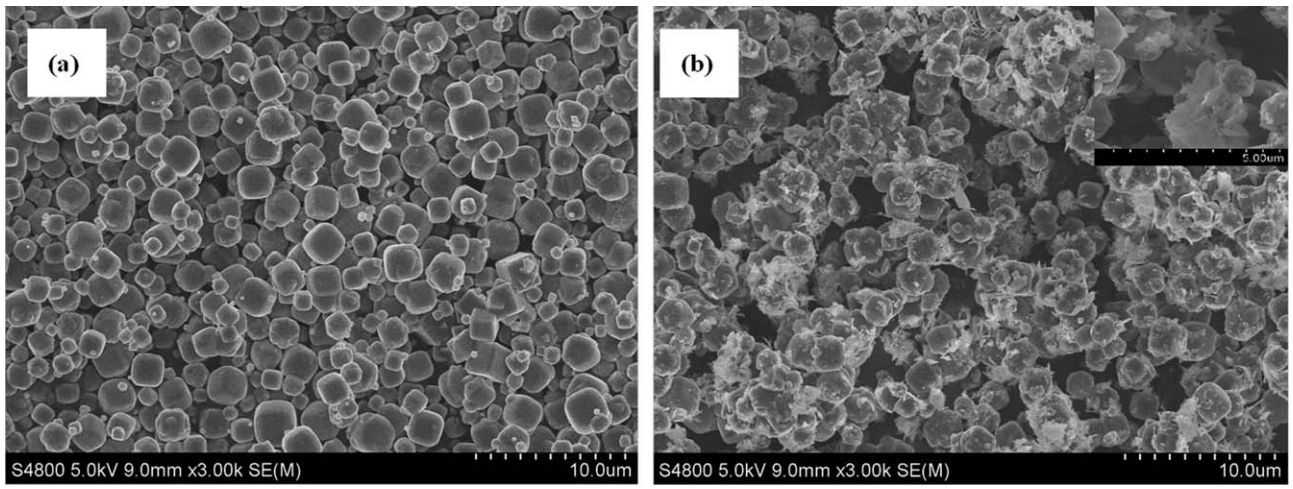

Figure 2. SEM graphs of zeolite samples prepared by two different methods (1 $\mu m = 10^{-6}$ m).

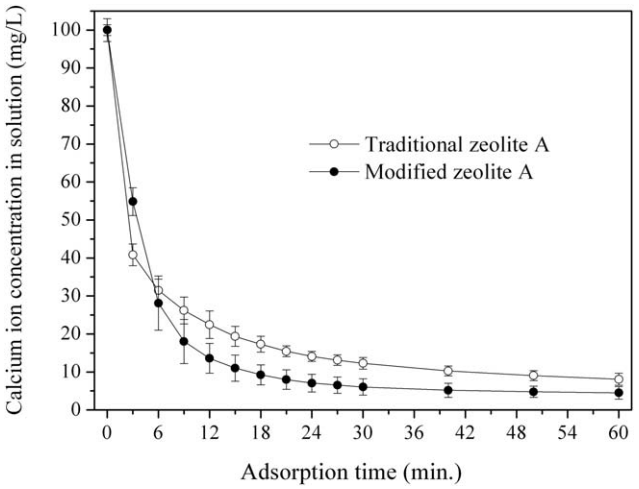

Figure 4. The change of calcium ion concentration with the adsorption time (1 mg/L = 10^{-3} kg/m^3; 1 min = 60 s).

reason could be ascribed to that the existence of lots of lamellate and needle-like crystals of the modified zeolite A was in favor of penetrating of calcium ions into pores and cages of the zeolite and exchanging easily with sodium ions in the pore channels and on the surface crystal layers. As shown in Figure 4, the calcium ion concentration in solution is below 5.0 mg/L, and the calcium ion removal efficiency gets up to 95.0% with the RSD of 1.45% after 1 h. Although, the calcium ion removal efficiency of the traditional zeolite A is 92.0% with the RSD of 1.74%. Moreover, the F inspection was used to analyze the variance of the adsorption amounts of the two zeolites. The results showed that the significant difference of the adsorption amounts reached at the 5% significant level after 24 min of the adsorption time. The calcium removal efficiency of the traditional zeolite A was lower than that of the modified zeolite A. This indicated that calcium ions could not penetrate thoroughly into the cages and pore channels of the zeolite to exchange with sodium ions, and also meant that diffusion resistance played an important role in the overall transport of the ions.[17] Similarly, in the research of the adsorption of mercuric and chromic ions from aqueous solutions onto activated carbon, McKay et al. found that the adsorption capacities showed a slightly particle size dependence possibly due to that the solute molecules or ions could not completely penetrate all the pores within the carbon particles.[41]

Adsorption kinetics

Pseudo-First-Order Rate Model. The plots of the pseudo-first-order rate equation fitting the experimental data are presented in Figure 5. The slopes and intercepts of the plots were used to determine the adsorption rate constants and the theoretical equilibrium adsorption capacities, respectively. The corresponding values are shown in Table 1. Obviously, for the modified zeolite A, the pseudo-first-order rate equation did not fit well the experimental data in the whole stage of the adsorption process from the view of linear correlation coefficient ($R^2 = 0.953$). Furthermore, the calculated theoretical adsorption capacity was significantly less than the experimental adsorption capacity. For the traditional zeolite A, although the experimental data could be fitted well with the pseudo-first-order rate equation, the calculated adsorption capacity still had a marked difference with the experimental value. Accordingly, the adsorption rates of the two types of zeolites did not follow the pseudo-first-order rate model.

Pseudo-Second-Order Rate Model. For pseudo-second-order rate model, the straight line plots of t/q_e against t (as shown in Figure 6) were also drawn to determine the parameters of the adsorption rate. The values of k_2, q_e, and correlation coefficient (R^2) for both types of the zeolites were calculated from the plots and presented in Table 1. It can be seen that the calculated adsorption capacities are very close to the experimental data for both types of the zeolites. Moreover, the correlation coefficients are both extremely high ($R^2 = 0.999$). This indicated that the experimental data could be fitted well with the pseudo-second-order equation, and the adsorption kinetics could be well described by pseudo-second-order rate model for both of the zeolites. Ho and McKay[25] also discovered that almost all of the literature systems previously reported including the adsorption of several metallic ions and other pollutants could be fitted well with the pseudo-second-order kinetic model, even though they could have been described by the pseudo-first-order rate model. As shown in Table 1, the adsorption rate constant of the modified zeolite A is 2.86 times more than that of the traditional zeolite A, indicating that the adsorption rate of the modified zeolite A is improved the same times under the same adsorption conditions. This further demonstrated that the existence of lamellate and needle-like crystals of the zeolite could reduce the diffusion distance of calcium ions into the pores of zeolite particles, facilitating ion exchange between calcium ions and sodium ions in the framework of the modified zeolite A.

Effect of Temperature on Adsorption Rate of Modified Zeolite A. The calcium ion removal performances of the modified zeolite A were investigated at the temperature from 298 to 313 K. The results are presented in Figure 7. Meanwhile, the estimated parameter values of the adsorption kinetics are listed in Table 2. As shown in Figure 7, it is apparent that temperature has a significant influence on the adsorption rate. The more the temperature increases, the steeper the curve of adsorption rate with the adsorption time. The experimental data were also fitted with the pseudo-second-order equation on the basis of the availability of the

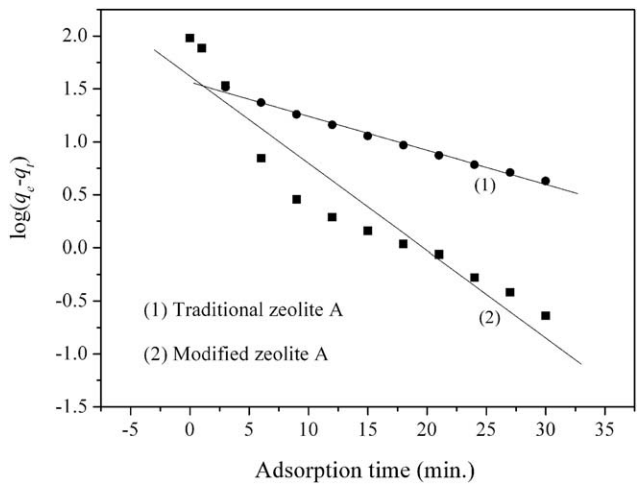

Figure 5. Lagergren pseudo-first-order rate model (1 min = 60 s).

Table 1. Parameters of Adsorption Rate with Different Adsorption Rate Equations (1 min^{-1}=1/60 s^{-1}; 1 g mg^{-1} min^{-1} = 50/3 kg kg^{-1} s^{-1}; 1 mg/g = 10^{-3} kg/kg)

Adsorption Rate Order	Temp. (K)	Zeolite	k	$q_{ecalc.}$[a] (mg/g)	$q_{eexp.}$[b] (mg/g)	R^2
Pseudo-first order	298	Traditional zeolite A	0.0741 min^{-1}	36.6	91.99	0.996
		Modified zeolite A	0.1896 min^{-1}	41.77	95.65	0.953
Pseudo-second order		Traditional zeolite A	0.00412 g mg^{-1} min^{-1}	95.4	91.99	0.999
		Modified zeolite A	0.01179 g mg^{-1} min^{-1}	98.33	95.65	0.999

[a]$q_{ecalc.}$ is the calculated equilibrium adsorption capacity.
[b]$q_{eexp.}$ is the experimental adsorption capacity.

kinetic model as discussed above. All of the linear correlation coefficients (R^2) of the linear plots of t/q_t vs. t at the temperature from 298 to 313 K were above 0.999. Moreover, as shown in Table 2, the adsorption rate constant is improved about 16 times at 313 K and three times at 303 K than that at 298 K, leading to t_{50} decreasing from 4 to 1.5 min and the equilibrium adsorption time t_{100} decreasing from 42 to 18 min with the increase of the adsorption temperature from 298 to 313 K, respectively. However, the calculated adsorption capacity decreases with the increase of the adsorption temperature, which is not in accordance with the trend of the experimental adsorption capacity. This may be ascribed to the experimental error and the calculation deviation resulting from the limitation of the linearization of the pseudo-second-order kinetic model.[42] The similar tendencies were also obtained by Ho[43] and Wang[35] in their researches of both adsorption of Acid Blue 25 onto peat and adsorption of methylene blue on modified ACFs at different temperatures.

Adsorption mechanisms

Effective Diffusion Coefficient Model and Surface Mass-Transfer Coefficient Model. For the effective diffusion coefficient model, the plots of Bt vs. t at the calcium ion concentration from 100 to 600 mg/L are presented in Figure 8. It can be seen that the plots of Bt vs. t at the calcium ion concentration less than 250 mg/L are not linear and do not pass through the origin, indicating that the adsorption processes are controlled by film diffusion in the studied conditions. The main reason of this phenomenon could be attributed to the very low calcium ion concentration, the small particle size, the relatively high affinity between adsorbate and adsorbent and the low adsorption temperature.[29,44] The adsorption mechanism might change depending on the variation of the rate-controlling step when these parameters and adsorption conditions changed. When the calcium ion concentrations are greater than 250 mg/L, the plots of Bt vs. t present straight lines passing through the origin with all of the linear correlation coefficients greater than 0.99, indicating that the adsorption processes are governed by intraparticle diffusion. Similar observations were also reported by El-Kamash et al.[18] in the research of zinc and cadmium ions removal from waste solutions and by El-Nagar et al.[16] in the research of Cesium and Strontium ions removal from aqueous solutions, respectively. The adsorption processes were both controlled by intraparticle diffusion when the concentrations of each studied ions were larger than 500 mg/L.

Moreover, the values of effective diffusion coefficient in the intraparticle diffusion governed stage were calculated according to the slopes of the fitting straight lines ($B=\frac{\pi^2 D_i}{r_0^2}$) and presented in Table 3. The effective diffusion coefficient increases from 3.03×10^{-13} to 4.26×10^{-13} m^2/s with the increase of the initial calcium ion concentration, and the values are of the same order of magnitude. In addition, the adsorption rate and the magnitude of the diffusion coefficient are dependent on the nature of the adsorption process. For physisorption process, the magnitude of the diffusion coefficient ranges from 10^{-6} to 10^{-9} m^2/s; and for chemisorption process, the value ranges from 10^{-9} to 10^{-17} m^2/s.[45] The different magnitude ranges of the diffusion coefficients are attributed to the difference of the binding force between adsorbate and adsorbent. For physisorption, the weak boundness between the adsorbate and interior surface of adsorbent

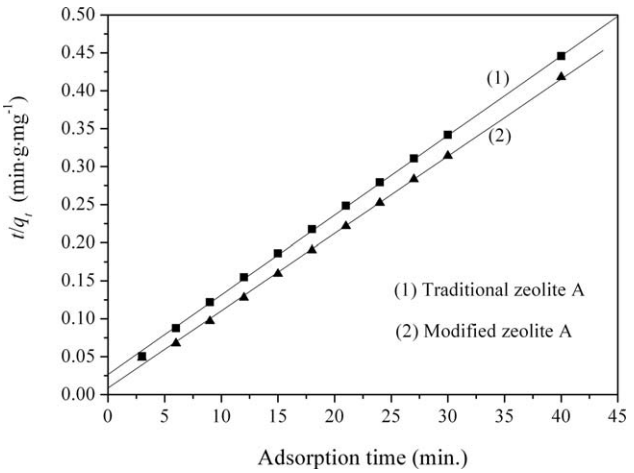

Figure 6. Lagergren pseudo-second-order rate model (1 min g mg^{-1} = 6 × 10^4 s kg kg^{-1}; 1 min = 60 s).

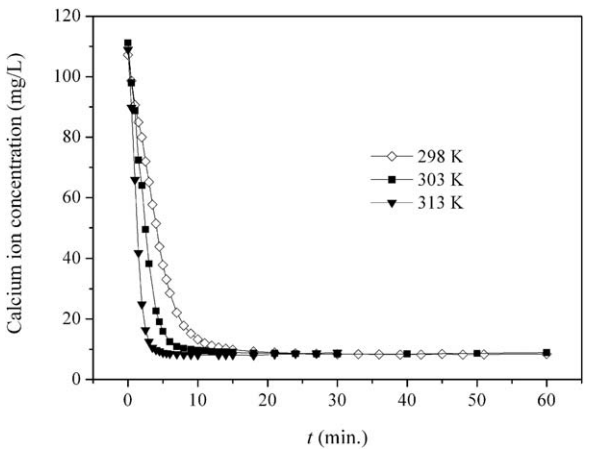

Figure 7. Calcium ion removal performances of modified zeolite A at the temperature from 298 to 313 K (1 mg/L = 10^{-3} kg/m^3; 1 min = 60 s).

Table 2. Effects of Temperature on the Kinetic Parameters (1 g mg^{-1} min^{-1} = 50/3 kg kg^{-1} s^{-1}; 1 mg/g = 10^{-3} kg/kg; 1 min = 60 s)

Temp. (K)	k_2 (g mg^{-1} min^{-1})	$q_{ecalc.}$[a] (mg/g)	$q_{eexp.}$[b] (mg/g)	R^2	t_{50} (min)[c]	t_{100} (min)[d]
298	0.00783	96.62	91.1	0.999	4	42
303	0.02390	93.37	91.6	0.999	2.5	30
313	0.12608	91.91	92.4	0.999	1.5	18

[a] $q_{ecalc.}$ is the calculated equilibrium adsorption capacity.
[b] $q_{eexp.}$ is the experimental adsorption capacity.
[c] The time required for reaching to fifty percent of equilibrium adsorption capacity.
[d] The time required for reaching to one hundred percent of equilibrium adsorption capacity.

makes the adsorbate migrate easily. Whereas, for chemisorption, the adsorbate is strongly bound and localized.[17,18]

For the surface mass-transfer coefficient model, if the adsorption process is governed by film diffusion, a plot of $\ln[C_t/C_0 - 1/(1+mK)]$ vs. t will yield a straight line as $t \to 0$, otherwise it is controlled by intraparticle diffusion.[33] It should be emphasized that only the adsorption process follows the assumption of the three-step model (including film diffusion, adsorption at an exterior site and intraparticle diffusion) and the intraparticle diffusion is assumed rapid with respect to the other two processes, then the process is controlled by film diffusion. The mass-transfer coefficient model had been used by Mohan et al. to study the adsorption mechanisms of both the adsorption of cadmium and zinc[44] and the adsorption of mercury[27] using activated carbon. However, it was not exact to fit the model linearly to the experimental data for the whole adsorption processes in our opinion. The reason was ascribed to dissatisfaction of the assumption of the model, and that the adsorption process was not merely controlled by the film diffusion in the whole period of adsorption. Only for the adsorption time, $t \to 0$ or at the initial period of adsorption, the surface mass transfer will predominate and the assumptions of the mass transfer of adsorbate from the bulk liquid to the particle surface and of the adsorption at an exterior site will be valid. This is further

Table 3. Parameters of the Mass Transfer Process of Calcium Ions (1 mg/L = 10^{-3} kg/m^3; 1 cm/s = 10^{-2} m/s)

C_0 (mg/L)	D_0 (m^2/s)	β_L (cm/s)
100	–	2.80×10^{-4}
150	–	1.21×10^{-4}
200	–	1.13×10^{-4}
250	3.03×10^{-13}	8.13×10^{-5}
300	3.21×10^{-13}	7.78×10^{-5}
400	3.23×10^{-13}	6.41×10^{-5}
500	3.89×10^{-13}	4.91×10^{-5}
600	4.26×10^{-13}	2.23×10^{-5}

verified in our research as shown in Figure 9. At any calcium ion concentration discussed, the value of $\ln[C_t/C_0 - 1/(1+mK)]$ does not change linearly as adsorption time increases within the whole adsorption period. However, at the initial stage of adsorption (0–150 s), the inset shows good linear relationship between the values of $\ln[C_t/C_0 - 1/(1+mK)]$ and the adsorption time, indicating that the adsorption process is controlled by the film diffusion and the applicability of the diffusion model. Consequently, the values of the mass-transfer coefficient at different calcium ion concentrations were calculated from the plots of $\ln[C_t/C_0 - 1/(1+mK)]$ vs. t with the intercept $mK/(1+mK)$ and the slope $-[(1+mK)/mK]\cdot\beta_L S_s$ at $t = 0$. As shown in Table 3, the values of β_L range from 2.23×10^{-5} to 2.80×10^{-4} cm/s, and decrease with the increase of the calcium ion concentration. The values of the surface mass-transfer coefficient were generally greater than that of the adsorption of most bivalent ions (shown in Table 4), demonstrating that the adsorption process was rapid. Meanwhile, it was foreseeable that the surface mass-transfer coefficient would increase to a considerable degree with the increase of the adsorption temperature based on the McKay'sconclusions.[33]

Change of pH Value of Solution with Adsorption Time. The effects of the initial pH value of solution on the adsorption capacity, kinetic adsorption curve, as well as hydroxyl complexes had been discussed in the processes of the

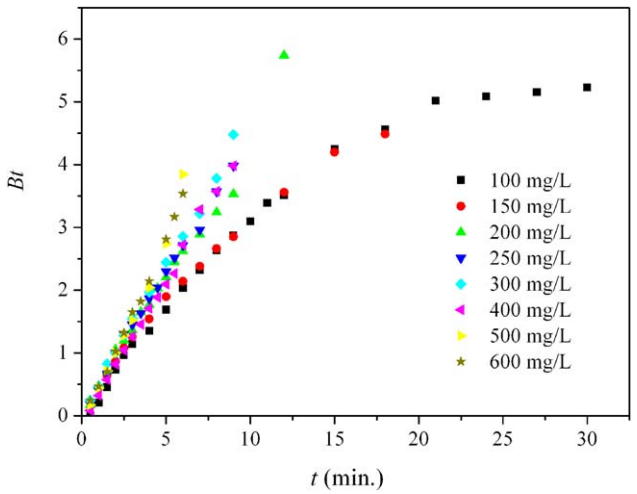

Figure 8. The plot of *Bt* vs. *t* at different concentration of calcium ions (1 mg/L = 10^{-3} kg/m^3; 1 min = 60 s).

[Color figure can be viewed in the online issue, which is available at wileyonlinelibrary.com.]

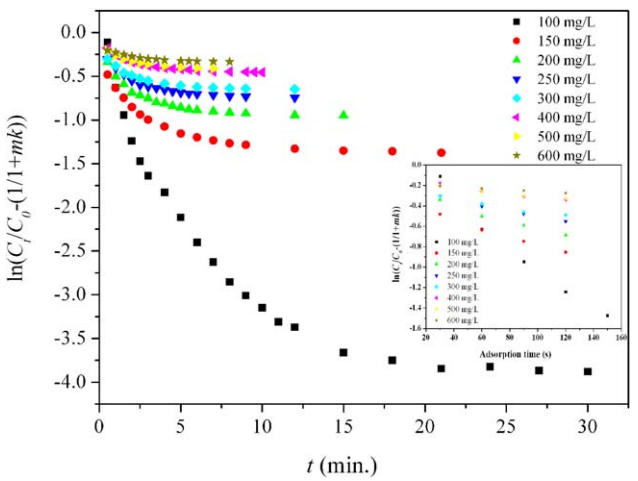

Figure 9. The plot of $\ln[C_t/C_0 - 1/(1+mK)]$ vs. adsorption time *t* (1 mg/L = 10^{-3} kg/m^3; 1 min = 60 s).

[Color figure can be viewed in the online issue, which is available at wileyonlinelibrary.com.]

Table 4. Comparison of Adsorption Property Parameters in Different Adsorption Processes

Adsorbent	Solution	Adsorbate	pH	Adsorption Temperature (K)	Adsorption Capacity	Effective Diffusion Coefficient (D_i; m^2/s)	Mass Transfer Coefficient (β_L; cm/s)	Reference
Graft copolymer	$CaCl_2$	Ca^{2+}	6	298 ± 0.5	20 mg/g	–	–	8
Ca-selectivity zeolite (A type)	$CaCl_2$	Ca^{2+}	12.5	293	105 mg/g	–	–	9
Zeolite A	$ZnCl_2$	Zn^{2+}	–	298	2.53 mmol/g	1.83×10^{-12}	–	18
	$PdCl_2$	Pd^{2+}			1.65 mmol/g	3.35×10^{-12}	–	
Zeolite A	CsCl	Cs^+	6.0	298	207.47 mg/g	6.45×10^{-12}	–	17
	$SrCl_2$	Sr^{2+}			303.00 mg/g	6.50×10^{-12}	–	
Zeolite A	CsCl	Cs^+	9±1	298	61.0 mg/g	5.40×10^{-12}	–	16
	$SrCl_2$	Sr^{2+}			146.86 mg/g	8.10×10^{-12}	–	
Mesoporous zeolite LTA	$CaCl_2$	Ca^{2+}	–	308	108.8 mg/g	–	–	21
Actived carbon (AC)	$Hg(NO_3)_2$	Hg^{2+}	2.0	300	3.2 mmol/g	4.54×10^{-10}	1.82×10^{-5}	27
Actived carbon (AC)	$Cd(NO_3)_2$	Cd^{2+}	4.5	298	38.03 mg/g	1.67×10^{-11}	1.124×10^{-5}	44
	$Zn(NO_3)_2$	Zn^{2+}			31.11 mg/g	2.17×10^{-11}	1.163×10^{-5}	
Wollastonite	$FeSO_4$	Fe^{2+}	4.0	303	0.4333 mg/g	4.00×10^{-11}	0.9993×10^{-5}	46
Modified zeolite A	$CaCl_2$	Ca^{2+}	5.5–6.0	298 ± 0.5	129.3 mg/g	$(3.03–4.26) \times 10^{-13}$	$(2.23–28.0) \times 10^{-5}$	This work
Modified zeolite A	Geothermal water[c]	Ca^{2+}	7.5	298 ± 0.5	69.8 mg/g	–	–	
Traditional zeolite A		Ca^{2+}	7.5	298 ± 0.5	62.2 mg/g	–	–	
13X zeolite[a]		Ca^{2+}	7.5	298 ± 0.5	42.4 mg/g	–	–	
Sodium bentonite[b]		Ca^{2+}	7.5	298 ± 0.5	4.44 mg/g	–	–	

(1 mg/g = 10^{-3} kg/kg; 1 mmol/g = 1 mol/kg; 1 cm/s = 10^{-2} m/s; 1 mg/L = 10^{-3} kg/m^3)
[a]13X was purchased from the Catalyst Plant of Nankai Unviersity in China.
[b]The bentonite was provided by Jilin Liufangzi Bentonite Technology, in China.
[c]The initial calcium ion concentration was 102.6 mg/L.

adsorption of Fe(II)/Fe(III), Cd(II), and methylene blue.[46–48] However, the pH is not invariable during adsorption process. So it has special significance to investigate the pH change during the adsorption process for further insight into the adsorption mechanism. The changes of pH values after adding the modified zeolite A into the $CaCl_2$ solution with the calcium ion concentration of 100 mg/L and into the deionized water are presented in Figure 10. The pH values increase dramatically after adding the adsorbents at the initial stage, then glide to different extents for both of the solutions. There were two main factors that affected the change of pH value: one was that the modified zeolite A possessed alkalinity, which could increase the pH value readily, and another was the ion-exchange reaction between the sodium ions in the zeolite and the hydrogen or calcium ions in the solution, which also made the pH value increase slightly. This resulted in a steep rise of the pH value from 5.5 to 9.0. In particular, the pH value changed significantly for the deionized water. Simultaneously, the zeolite inevitably underwent weak hydrolysis in aqueous solution, accompanying the increase of the hydrogen ion concentration. This made the pH value of the solution decline with the extending of the whole mixing time.[20] Nevertheless, the pH value of the $CaCl_2$ solution declined more apparently due to the complexation between hydroxyl ions and calcium ions near or on the surface of the zeolite particles such as the reaction equations provided in formula (19) and (20). Accordingly, the adsorption process included not only the ion-exchange mechanism but also the complexation process between the calcium ions and the hydroxyl ions.[9,49] This would result in higher adsorption free energy compared with that of the simple ion-exchange process[50]

$$Ca^{2+} + OH^- \rightarrow Ca(OH)^+ \quad (19)$$

$$Ca^{2+} + 2OH^- \rightarrow Ca(OH)_2 \quad (20)$$

Adsorption isotherms

Adsorption Equilibrium at Different Temperatures. The adsorption equilibrium data at the temperature from 298 to 353 K are shown in Figure 11. As shown in the plots, the calcium ion concentrations increase gradually from 80 to 800 mg/L at different temperatures. The adsorption amounts increase with the increase of the calcium ion concentration at any fixed adsorption temperature. This might be due to the progressive surface coverage and the filling of pores of

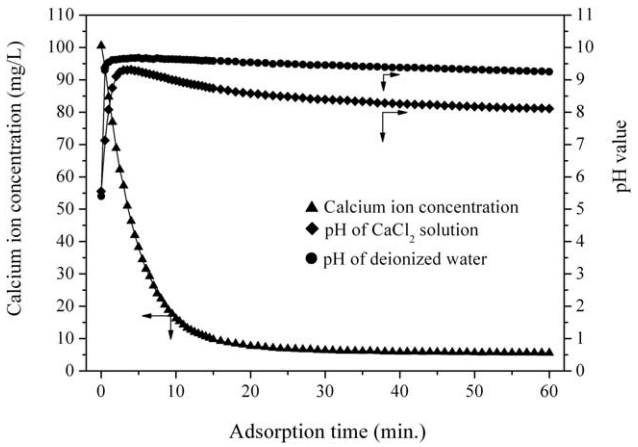

Figure 10. The changes of pH value and calcium ion concentration of solution with the adsorption time (1 mg/L = 10^{-3} kg/m^3; 1 min = 60 s).

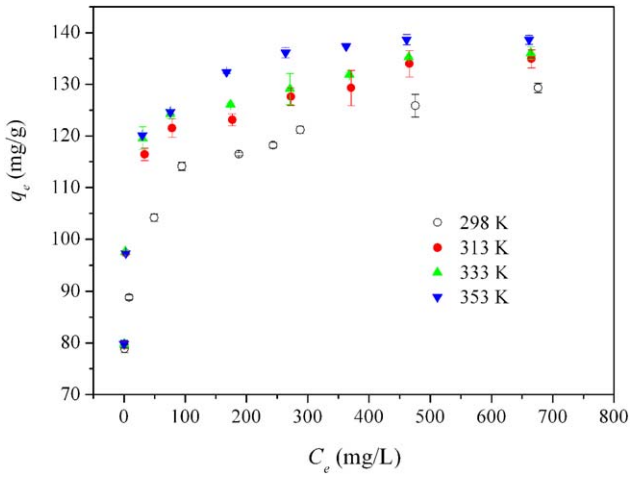

Figure 11. The experimental data of adsorption equilibrium at the temperature from 298 to 353 K (1 mg/g = 10^{-3} kg/kg; 1 mg/L = 10^{-3} kg/m^3).

[Color figure can be viewed in the online issue, which is available at wileyonlinelibrary.com.]

the zeolite particles with calcium ions. Thus, the collision probability between calcium ions and sodium ions in the framework of zeolite increased, and more calcium ions were exchanged into the adsorbent. Although, the increasing tendency recedes gradually, at last reaches to a platform because of achieving the absorption equilibrium at the respective temperature. The isotherm is a function of temperature and normality, and the ultimate equilibrium adsorption capacity is constant at a given temperature.[51] Accordingly, the equilibrium adsorption capacities increase from 129.3 to 138.6 mg/g as the adsorption temperature increases from 298 to 353 K. One reason was that the degree of ion exchange between calcium ions and sodium ions in the cages of the zeolite was improved at higher temperature, leading to the increase of the active exchange sites available for ion exchange. Another reason might be due to the change in pore size of zeolite and the improvement of intraparticle diffusion rate of solute as diffusion was an endothermic process.[52] Similarly, the increasing tendency gradually decreased to a certain value, due to the limitation of the maximum exchange level for the ion-exchange cases.[38,51] Moreover, the ending pH values of the solutions with the calcium ion concentration of 800 mg/L were in the range from 7.45 to 7.62 at the adsorption temperature from 298 to 353 K. There was no significant difference for ending pH values at different adsorption equilibrium states, because there was only 7.19% of difference in calcium adsorption amount at the adsorption temperature between 298 and 353 K. Besides, the modified zeolite A had obviously higher adsorption capacity for calcium ion compared with other adsorbents as shown in Table 4.

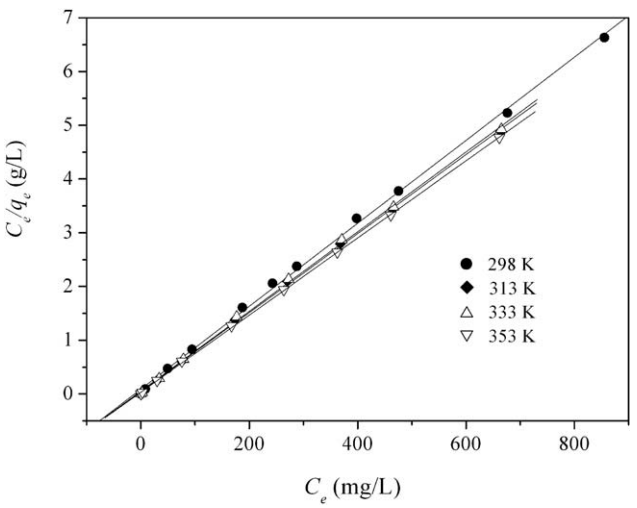

Figure 12. The Langmuir isotherm plots for calcium ion adsorption with the modified zeolite A at the temperature from 298 to 353 K (1 g/L = 1 kg/m^3; 1 mg/L = 10^{-3} kg/m^3).

Table 5. The Calculated Parameters of Langmuir Equation (1 mg/g = 10^{-3} kg/kg; 1 L/mg = 10^3 m^3/kg)

T (K)	Q_0 (mg/g)	b (L/mg)	R^2
298	129.530	0.08792	0.9994
313	134.953	0.135367	0.9995
333	136.054	0.162791	0.9997
353	139.276	0.217509	0.9999

Langmuir Adsorption Isotherm. The experimental data obtained at the temperature from 298 to 353 K were fitted by the linear form of Langmuir equation. The plots of C_e/q_e against C_e at different temperatures are shown in Figure 12. The slopes $1/Q_0$ and the intercepts $1/Q_0b$ of the each plot were used to estimate the values of the maximum adsorption capacity Q_0 and the Langmuir constant b, respectively. The values of these parameters and the linear correlation coefficients are listed in Table 5. It can be seen that the Langmuir equation fits the experimental data with high correlation coefficients ($R^2 > 0.999$) in the whole ranges of studied concentrations and temperatures. The estimated values of Q_0 (in Table 5) are very close to the experimental data (shown in Figure 12), corresponding to the monolayer coverage. This further confirms that the expression of Langmuir equation is a reasonable representation of chemisorption isotherm.[17] In addition, the maximum adsorption capacity increases with the increase of the temperature, indicating that the adsorption of calcium ions onto the modified zeolite A is endothermic process. The same tendency was observed for the values of Langmuir constant, which demonstrated that the adsorption intensity strengthened as the temperature increased. This was corresponding with the nature of the ion-exchange adsorption process.

D–R and D–A Isotherm Models. Based on the D–R model, from the experimental equilibrium data obtained at different temperatures, the plots of ln q_e against ε are presented in Figure 13. The values of q_m and β were estimated from the intercepts and slopes of the plots in the temperature range of 298 to 353 K. The values of q_m, β, and E, together with the linear correlation coefficients are shown in Table 6. From the view of the linear correlation coefficient, the D–R model can fit well the experimental points at any investigated temperature. Simultaneously, the magnitudes of E at all of the investigated temperatures are larger than 16 kJ/mol, indicating that other interactions such as surface precipitation or coprecipitation occur along with the ion-exchange phenomenon in the adsorption system.[37,51] This is corresponding with the conclusion obtained from the pH change of solution. The values of maximum adsorption capacity, q_m are all remarkably larger than the experimental values at the

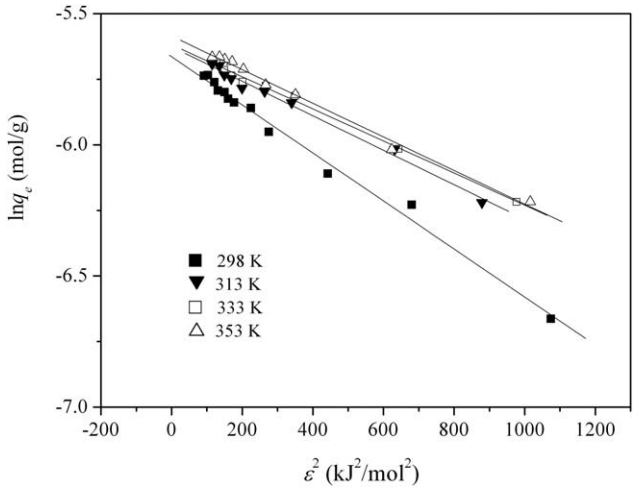

Figure 13. The D–R isotherm plots for calcium ion adsorption with the modified zeolite A at the temperature from 298 to 353 K (1 mol/g = 10^3 mol/kg; 1 kJ^2/mol^2 = 10^6 J^2/mol^2).

corresponding temperature, although it has provided the same rising tendency of adsorption capacity with temperature. The similar results were also observed by Dron and Dodi in the researches of Cl^-, NO_3^-, and SO_4^{2-} removals from aqueous solutions by an anion exchange resin.[53] Thus, the values of q_m deduced from the D–R model could not be veritably representative of the maximum adsorption capacity. The obvious deviations of the adsorption capacities and the slightly anomalous values of the adsorption free energies at different temperatures were mainly attributed to the defect of D–R model, in which the heterogeneity parameter of the adsorbent (the exponential term of linearized the D–R equation) was arbitrarily defined as 2. Actually, there is a significant difference of the values of the heterogeneity parameter for different adsorbents. Moreover, the values change with the pore structure and the surface physicochemical property of the adsorbents. Inglezakis[51] also pointed out that the value of heterogeneity parameter was strongly influenced by the structure of the adsorbent and in lesser extent by the cation exchanged in the research of the ion exchange of Pb^{2+} in the zeolite clinoptilolite.

For the application of the D–A equation, the maximum exchange capacity should be determined in the system, and the critical parameter commonly was measured using the repeated equilibrations method.[38,51] Although, the disparity between surface coverage and pore filling, monolayer and multilayer coverage is not clear for the ion exchange system, because the ion exchange is a stoichiometric phenomenon.[51] Therefore, the maximum exchange capacity (q_m) is corresponding to Q_0 in the Langmuir model, which also has been adopted in our adsorption systems.[38,51,53,54]

Based on the experimental equilibrium data and the obtained values of Q_0 in the Langmuir model at different temperatures, the D–A model was forced to fit the experimental data to determine the values of heterogeneity parameter (n) and adsorption free energy (E) using the software Statistica 8.0, by means of the nonlinear regression analysis with least square method. The calculated values are listed in Table 6. It is obvious that all of the values of adsorption free energy at the temperature from 298 to 353 K are considerably larger than 16 kJ/mol. This firmly demonstrates that the process is accompanying with the complexation except for the ion-exchange process once again. Inglezakis[51] also noted that the adsorption energy of Na-rich clinoptilolite was somewhat higher than that of the natural sample. Moreover, the vales of adsorption free energy increase from 23.4 to 30.3 kJ/mol as the adsorption temperature increases, indicating the enhancement of the interaction between the calcium ions/hydroxyl calcium and the surface of the zeolite. As shown in Table 6, the values of heterogeneity parameter are noticeable larger than 2 adopted in the D–R model, demonstrating more homogeneity of the pore structure of the zeolite adsorbent compared with carbon.[55]The more homogeneous the pores, the greater its value is.[51,56] Although, it was yet not corresponding to the values of n greater than 3–4 as expected,[37] might be due to the characteristics of the zeolite processing lots of lamellate and needle-like crystals. Furthermore, the heterogeneity parameter was almost not affected by the adsorption temperature and around the value of 2.8 with the exception of the value of 2.55 at the temperature of 298 K. The deviation might be induced by the experiment errors because of the slightly lower value of the nonlinear correlation coefficient. Therefore, this was in agreement with the conclusion that the heterogeneity parameter was a function of properties of both adsorbent and adsorbate, and more influenced by the structure of the adsorbent. In conclusion, when combined with the Langmuir model, the D–A model could appropriately describe the adsorption free energy, the nature of adsorption, the pore structure and surface physicochemical property of the adsorbent by means of the value of adsorption energy, the equilibrium adsorption capacity and the heterogeneity parameter of adsorbent.

Thermodynamic parameters

Thermodynamic studies should be carried out to illustrate whether the ion-exchange adsorption process is spontaneous or not. The thermodynamic parameters including the

Table 6. The Parameters of D–R and D–A Equations (1 mol^2/kJ^2 = 10^{-6} mol^2/J^2; 1 mg/g = 10^{-3} kg/kg; 1 kJ/mol = 10^3 J/mol)

	D–R Model Parameters				D–A Model Parameters			
T (K)	β (mol^2/kJ^2)	q_m (mg/g)	E (kJ/mol)	R^{2a}	q_m (mg/g)^b	E (kJ/mol)	n	R^{2c}
298	9.1555×10^{-4}	138.65	23.37	0.995	129.53	23.40	2.55	0.972
313	6.5742×10^{-4}	144.08	27.58	0.995	134.953	26.26	2.82	0.992
333	6.1158×10^{-4}	145.21	28.59	0.998	136.054	29.00	2.82	0.993
353	6.4037×10^{-4}	150.05	27.943	0.997	139.276	30.31	2.89	0.983

[a]The value of R^2 in D–R model represents the linear correlation coefficient.
[b]The maximum adsorption capacity obtained based on the Langmuir model.
[c]The value of R^2 in D–A model represents the nonlinear correlation coefficient obtained based on least square method.

Table 7. The Calculated Values of the Thermodynamic Parameters of the Adsorption Process (1 kJ/mol = 10^3 J/mol)

T (K)	K_c	ΔG^0(kJ/mol)	ΔH^0(kJ/mol)	ΔS^0(J/(mol K))
298	11.388	−6.027	14.679	70.079
313	18.268	−7.198		
333	22.148	−7.675		
353	30.294	−8.451		

standard enthalpy change (ΔH^0), the standard entropy change (ΔS^0), and the standard free energy (ΔG^0) should be calculated to determine the process. These parameters can be calculated through the equations as follows

$$\Delta G^0 = -RT \ln K_c \tag{21}$$

$$\Delta G^0 = \Delta H^0 - T\Delta S^0 \tag{22}$$

$$\ln K_c = \frac{\Delta S^0}{R} - \frac{\Delta H^0}{RT} \tag{23}$$

where K_c is the equilibrium constant, R is the ideal gas constant. The application of the equation 23 is based on the assumption that ΔH^0 and ΔS^0 do not change detectably with the increase of the adsorption temperature.

Ion exchange is not a chemical reaction and occurs, as a rule, with little increase or decrease of enthalpy and entropy.[28] Hence, ΔH^0 and ΔS^0 can be calculated from the temperature dependence of the equilibrium constant by use of the equations 21–23. In addition, we noticed that the different values (including the value of the parameter b[44,51,57,58] or $Q_0 b$[17,59,60] in Langmuir model) were used to obtain the value of equilibrium constant to calculate the values of ΔG^0 in several literatures. This would lead to the deviation of the calculated values of the thermodynamic parameters. In fact, from the point of view of the definition the equilibrium constant should be the ratio of the amount of adsorbate adsorbed on the adsorbent per liter to the equilibrium concentration of the adsorbate in solution.[59,61] Meanwhile, at low adsorbate concentration, the Langmuir Eq. 13 can be effectively reduced to a linear isotherm, and thus, the simplified equation follows Henry's law with the Henry's constant of $Q_0 b$.[60] Just like as declared by Pradaset al.[62] in the research of the adsorption of cadmium and zinc from aqueous solution on the natural and activated bentonite, the parameter b could not be taken into account as an indicator, not even relative,

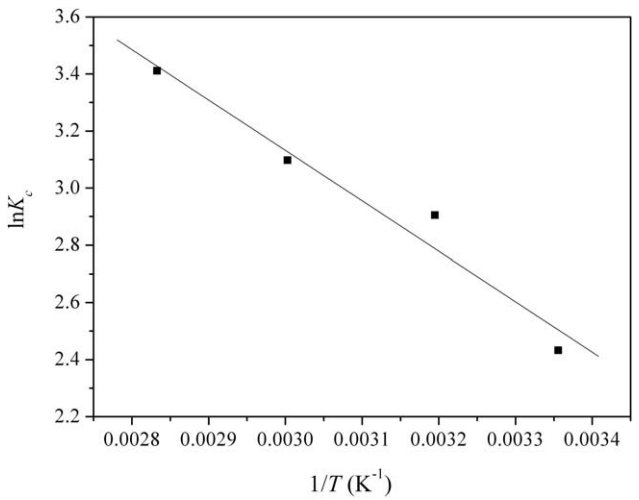

Figure 14. The plot of ln K_c vs. 1/T.

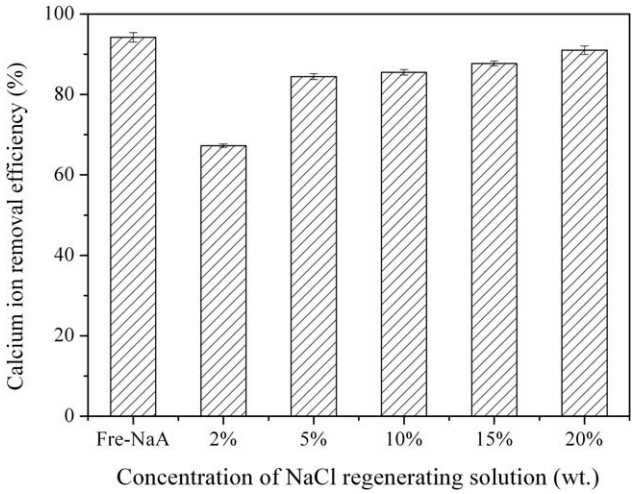

Figure 15. The calcium ion removal efficiencies of the regenerated zeolites with different concentrations of sodium chloride solutions.

of the affinity for the divalent cations. As known, a relative indicator of the affinity for the divalent cations (when the experiment data are fitted with the Langmuir equation) is the apparent equilibrium constant, K_c, which may be calculated as the product of b and Q_0. Hence, the values of K_c at different temperatures were replaced by the product of the parameters b and Q_0 in the calculation, which were more appropriate in our opinion. The calculated values of the parameters K_c and ΔG^0 are listed in Table 7. Simultaneously, the values of ΔH^0 and ΔS^0 were calculated from the slope and the intercept of the linear plot of $\ln K_c$ vs. $1/T$ (Figure 14), respectively. Both of the values are also presented in Table 7. It can be seen that the equilibrium constant increases from 11.388 to 30.294 with the increase of the adsorption temperature from 298 to 353 K. This indicates that the adsorption affinity of the calcium ions onto the zeolite strengthens with the increase of the temperature. The value of ΔG^0 is negative and decreases from −6.027 to −8.451 kJ/mol with the increase of the temperature, demonstrating that the adsorption process is spontaneous and more energetically favorable at higher temperature. Furthermore, the calculated values of ΔH^0 and ΔS^0 are 14.679 kJ/mol and 70.079 J/(mol·K), respectively. The positive value of ΔH^0 showed that the adsorption process was endothermal in nature, and the positive value of ΔS^0 reflected an irregular increase of the randomness at the zeolite solid/solution interface during the adsorption process.[17,58,61]

Calcium ion removal efficiency of regenerated zeolite A

To investigate the reusability of the modified zeolite A, the regeneration of the zeolite adsorbed and saturated by $CaCl_2$ solution was carried out with different concentrations of NaCl solutions. The calcium ion removal efficiencies of the regenerated zeolites are presented in Figure 15. The calcium ion removal efficiency increases from 67.3% to 91.0% with the increase of the NaCl concentration from 2 wt % to 20 wt %. In the regeneration process of the zeolite saturated by calcium ions, the NaCl concentration gradient close to the particle surface of the zeolite increased with the increase of the NaCl concentration. The extent of the ion-exchange process of sodium ions instead of calcium ions in the zeolite at higher NaCl concentration was greater than that at lower

Table 8. The Main Composition of Geothermal Water of a Geothermal Well in Tianjin, China[a] (1 mg/L = 10^{-3} kg/m^3)

Entry	Conc. (mg/L)	Entry	Conc. (mg/L)	Entry	Conc. (mg/L)
Na^+	461.6	SO_4^{2-}	319.4	Soluble SiO_2	64.5
K^+	71.2	HCO_3^-	393.6	TDS	1797.2
Ca^{2+}	102.6	Cl^-	528.8	pH	7.52
Mg^{2+}	12.2	NO_3^-	12.54	–	–

[a]The calcium ion concentration in Table 8 was detected by the EDTA titration method before the experiment, and the contents of other constituents were obtained from the evaluation report of Tianjin geothermal resources.

NaCl concentration.[23] Thus, the zeolite A regenerated with 20 wt % NaCl solution presented the highest calcium ion removal efficiency. The high calcium ion removal efficiency of the regenerated zeolite approaching to that of the freshly modified zeolite A (about 94.2%) demonstrated that the ion-exchange adsorption process was a reversible process.[63] Moreover, in the range of the lifetime of hydrothermal stability of zeolite,[64] the modified zeolite A possessed the reversible ion exchange ability.

Calcium removal performance of modified zeolite A from geothermal water

The change of calcium ion concentration before and after the adsorption process with the modified zeolite A for the geothermal water taken from a geothermal well in Tianjin, China was investigated. The main composition of the geothermal water is listed in Table 8. The calcium ion concentration in the geothermal water after the adsorption was 32.8 mg/L. The calcium ion adsorption amount was 69.8 mg/g, and the calcium ion removal efficiency was 68.03%. The calcium removal performances of the modified zeolite A in the geothermal water of different calcium ion concentrations are shown in Figure 16. When the calcium ion concentration is reduced to 17.5 mg/L, the calcium ion adsorption amount is 17.0 mg/g, and the calcium ion removal efficiency gets up to 97.56%. When the calcium ion concentration reaches to 1002.3 mg/L, the calcium ion adsorption amount gets up to 123.1 mg/g. However, the calcium ion removal efficiency from the geothermal water is only 12.29%. The calcium ion adsorption amount increases with the increase of the calcium ion concentration in geothermal water. However, the calcium ion removal efficiency decreases with the increase of the calcium ion concentration. The main reason was that the adsorption capacity of the modified zeolite A was 129.3 mg/g at 298 K as stated in the calcium adsorption process for the $CaCl_2$ solution, due to the limitation of the maximum exchange level. Furthermore, the adsorption capacity of the modified zeolite A in geothermal water was less than that in the single kind of solution of $CaCl_2$. The reason could be ascribed to that the competitive adsorption of coexisting ions affected the adsorption selectivity of the zeolite and the interference of ionic strength hindered the diffusion of calcium ions replacing sodium ions in the framework of the zeolite. The relatively higher adsorption capacity for calcium ions from geothermal water indicates that the modified zeolite A has a great potential application for descaling of geothermal water.

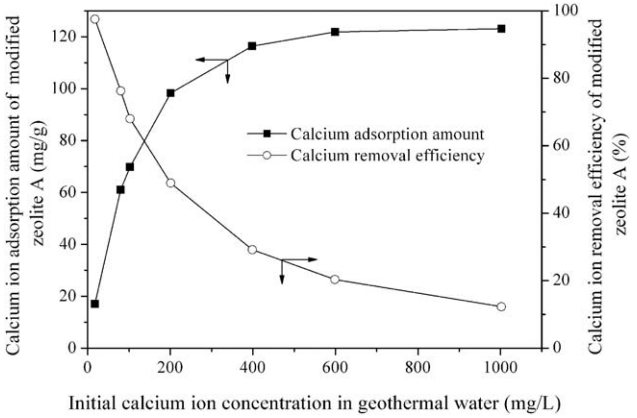

Figure 16. The calcium ion adsorption amount and calcium ion removal efficiency of modified zeolite A from geothermal water (1 mg/g = 10^{-3} kg/kg; 1 mg/L = 10^{-3} kg/m^3).

Concluding Remarks

The modified zeolite A showed high calcium ion removal efficiency from aqueous solution. The adsorption capacity was largely affected by calcium ion concentration and adsorption temperature. The adsorption rate was fitted well with the pseudo-second-order rate model. The adsorption process was controlled by film diffusion at low calcium ion concentration (<250 mg/L) while it was controlled by intraparticle diffusion at higher calcium ion concentration (>250 mg/L). The estimated values of effective diffusion coefficient indicated that the nature of the process belonged to chemisorption. The calculated mass-transfer coefficient decreased from 2.80×10^{-4} to 2.23×10^{-5} cm/s with the increase of calcium ion concentration from 100 to 600 mg/L. D–A model could appropriately describe the adsorption free energy, the nature of adsorption, the pore structure, and surface physicochemical property of the adsorbent when combined with Langmuir model. Moreover, the values of the heterogeneity parameter were noticeably larger than 2, and not significantly affected by the adsorption temperature.

The adsorption process was spontaneous and endothermal in nature, and included not only ion exchange but also complexation reaction between calcium and hydroxyl ions. The higher calcium adsorption capacity indicates that the modified zeolite A has a great potential application for scale removal from geothermal water. Even so, several aspects not clarified in this research, such as the adsorption coefficient in geothermal water, competitive adsorption mechanism, and utilization form of the zeolite, will be focused on in our further work.

Acknowledgments

The authors thank for the financial support of the National High-Tech Research and Development Projects of China ("863" Program, No. 2012AA052804). The authors are also grateful for the valuable advices on the research approach from Professor Shanrang Yang in Northeast Dianli Unviersity of China.

Literature Cited

1. Steinhagen R, Müller-Steinhagen H, Maani K. Problems and costs due to heat exchanger fouling in New Zealand industries. *Heat Transfer Eng.* 1993;14:19–30.
2. Siega FL, Herras EB, Buñing BC. Calcite scale inhibition: the case of Mahanagdong Wells in Leyte geothermal production field, Philippines. In: Proceedings of World Geothermal Congress, Antalya, Turkey, 2005.

3. Cho YI, Choi BG, Drazner BJ. Electronic anti-fouling technology to mitigate precipitation fouling in plate-and-frame heat exchangers. *Int J Heat Mass Transfer*. 1998;41:2565–2571.
4. Müller-Steinhagen H, Zhao Q. Investigation of low fouling surface alloys made by ion implantation technology. *Chem Eng Sci*. 1997; 52:3321–3332.
5. Minissale A, Borrini D, Montegrossi G, Orlando A, Tassi F, Vaselli O, Huertas AD, Yang J, Cheng W, Tedesco D, Poreda R. The Tianjin geothermal field (north-eastern China): water chemistry and possible reservoir permeability reduction phenomena. *Geothermics*. 2008;37:400–428.
6. Nefzi M, Ben Amor M, Maalej M. A clean technology for decarbonation of geothermal waters from Chott E1 Fejjej using a three-phase fluidized bed reactor-modelling aspects. *Desalination*. 2004;165:337–350.
7. Gallupa D, Sugiaman F, Capuno V, Manceau A. Laboratory investigation of silica removal from geothermalbrines to control silica scaling and produce usable silicates. *Appl Geochem*. 2003;18:1597–1612.
8. Furlan L, de Fávere VT, Laranjeira M. Adsorption of calcium ions by graft copolymer of acrylic acid on biopolymer chitin. *Polymer*. 1996;37:843–846.
9. Qin C, Wang R, Ma W. Characteristics of calcium adsorption by Ca-Selectivity zeolite in fixed-pH and in a range of pH. *Chem Eng J*. 2010;156:540–545.
10. Herrmann CC, Klein G. Zeolite Afor selective calcium removal from brackish water. *React Polym Ion Exch Sorbents*. 1987;5:281–293.
11. Ramdani A, Taleb S, Benghalem A, Ghaffour N. Removal of excess fluoride ions from Saharan brackish water by adsorption on natural materials. *Desalination*. 2010,250:408–413.
12. Qin C, Wang R, Ma W. Adsorption kinetic studies of calcium ions onto Ca-Selective zeolite. *Desalination*. 2010;259:156–160.
13. Coker EN, Rees LVC. Kinetics of ion exchange in quasi-crystalline aluminosilicate zeolite precursors. *Microporous Mesoporous Mater*. 2005;84:171–178.
14. Muraviev D, Khamizov RK, Tikhonov NA, Morales JG. Clean ("green") ion-exchange technologies. 4. High-Ca-selectivity ion-exchange material for self-sustaining decalcification of mineralized waters process. *Ind Eng Chem Res*. 2004;43:1868–1874.
15. Sivasankar V, Ramachandramoorthy T. Water softening behaviour of sand materials-Mimicking natural zeolites in some locations of Rameswaram Island, India. *Chem Eng J*. 2011;171:24–32.
16. El-Nagar MR, El-Kamash AM, Ghoneem AK. Kinetic studies on the removal of cesium and strontium ions from aqueous solutions using prepared zeolite-A. *Arab J Nucl Sci Appl*. 2005;38:91–101.
17. El-Kamash AM. Evaluation of zeolite A for the sorptive removal of $Cs^{+}$and Sr^{2+} ions from aqueous solutions using batch and fixed bed column operations. *J Hazard Mater*. 2008;151:432–445.
18. El-Kamash AM, Zaki AA, El Geleel MA. Modeling batch kinetics and thermodynamics of zinc and cadmium ions removal from waste solutions using synthetic zeolite A. *J Hazard Mater*. 2005;127:211–220.
19. Thompson RW, Huber MJ. Analysis of the growth of molecular sieve zeolite NaA in a batch precipitation system. *J Cryst Growth*. 1982;56:711–722.
20. Drummond D, De Jonge A, Rees L. Ion-exchange kinetics in zeolite A. *J Phys Chem*. 1983;87:1967–1971.
21. Xue Z, Ma J, Hao W, Bai X, Kang Y, Liu J. Li R. Synthesis and characterization of ordered mesoporous zeolite LTA with high ion exchange ability. *J Mater Chem*. 2012;22:2532–2538.
22. Fang S, Fu Y, Liu P. Application of an ion selective electrode to study in situ in kinetics of cations exchange in zeolite Y. *Talanta*. 1994;41:155–157.
23. Purna Chandra Rao G, Satyaveni S, Ramesh A, Seshaiah K, Murthy KSN, Choudary NV. Sorption of cadmium and zinc from aqueous solutions by zeolite 4A, zeolite 13X and bentonite. *J Environ Manage*. 2006;81:265–272.
24. Ho YS, McKay G. The sorption of lead (II) ions on peat. *Water Res*. 1999;33:578–584.
25. Ho YS, McKay G. Pseudo-second order model for sorption processes. *Process Biochem*. 1999;34:451–465.
26. Coleman NT, McClung AC, Moore DP. Formation Constants for Cu (II)-Peat Complexes. *Science*. 1956;123:330–331.
27. Mohan D, Gupta VK, Srivastava SK, Chander S. Kinetics of mercury adsorption from wastewater using activated carbon derived from fertilizer waste. *Colloid Surf A*. 2001;177:169–181.
28. Helfferich F. Ion Exchange. New York: McGraw-Hill Book Company, 1962.
29. Boyd GE, Adamson AW, Myers LS Jr. The exchange adsorption of ions from aqueous solutions by organic zeolites. II. Kinetics. *J Am Chem Soc*. 1947;69:2836–2848.
30. Helfferich F, Plesset MS. Ion exchange kinetics. A nonlinear diffusion problem. *J Chem Phys*. 1958;28:418.
31. Reichenberg D. Properties of ion-exchange resins in relation to their structure. *III. Kinetics of exchange. J Am Chem Soc*. 1953;75:589–597.
32. Mohan D, Singh KP, Sinha S, Gosh D. Removal of pyridine from aqueous solution using low cost activated carbons derived from agricultural waste materials. *Carbon*. 2004;42:2409–2421.
33. McKay G, Allen SJ, McConvey IF, Otterburn MS. Transport processes in the sorption of colored ions by peat particles. *J Colloid Interface Sci*. 1981;80:323–339.
34. Monazam ER, Shadle LJ, Miller DC, Pennline HW, Fauth DJ, Hoffman JS, Gray ML. Equilibrium and kinetics analysis of carbon dioxide capture using immobilized amine on a mesoporous silica. *AIChE J*. 2013;59:923–935.
35. Wang L, Huang Z, Zhang M, Chai B. Adsorption of methylene blue from aqueous solution on modified ACFs by chemical vapor deposition. *Chem Eng J*. 2012;189–190:168–174.
36. Vijayaraghavan K, Padmesh T, Palanivelu K, Velan M. Biosorption of nickel (II) ions onto Sargassum wightii: application of two-parameter and three-parameter isotherm models. *J Hazard Mater*. 2006;133:304–308.
37. Inglezakis VJ, Stylianou M, Loizidou M. Ion exchange and adsorption equilibrium studies on clinoptilolite, bentonite and vermiculite. *J Phys Chem Solids*. 2010;71:279–284.
38. Inglezakis VJ. The concept of "capacity" in zeolite ion-exchange systems. *J Colloid Interface Sci*. 2005;281:68–79.
39. Dubinin MM, Astakhov VA. Development of the concepts of volume filling of micropores in the adsorption of gases and vapors by microporous adsorbents. *Russ Chem Bull*. 1971;20:3–7.
40. Treacy MMJ, Higgins JB. Collection of Simulated XRD Powder Patterns for Zeolites, 4th Revised ed. Amsterdam: Elsevier Science Ltd, 2001.
41. McKay G, Bino MJ, Altamemi AR. The adsorption of various pollutants from aqueous solutions on to activated carbon. *Water Res*. 1985;19:491–495.
42. Cheung WH, Ng J, Mckay G. Kinetic analysis of the sorption of copper (II) ions on chitosan. *J Chem Technol Biotechnol*. 2003;78:562–571.
43. Ho YS, McKay G. Sorption of dye from aqueous solution by peat. *Chem Eng J*. 1998;70:115–124.
44. Mohan D, Singh KP. Single-and multi-component adsorption of cadmium and zinc using activated carbon derived from bagasse-an agricultural waste. *Water Res*. 2002;36:2304–2318.
45. Walker GM, Weatherley LR. Kinetics of acid dye adsorption on GAC. *Water Res*. 1999;33:1895–1899.
46. Singh AK, Singh DP, Panday KK, Singh VN. Wollastonite as adsorbent for removal of Fe (II) from water. *J Chem Technol Biotechnol*. 1988;42:39–49.
47. Periasamy K, Namasivayam C. Process development for removal and recovery of cadmium from wastewater by a low-cost adsorbent: adsorption rates and equilibrium studies. *Ind Eng Chem Res*. 1994; 33:317–320.
48. Esparza P, Borges ME, Díaz L, Alvarez-Galván MC, Fierro JLG. Equilibrium and kinetics of adsorption of methylene blue on Ti-modified volcanic ashes. *AIChE J*. 2011;57:819–825.
49. Mohamed RM, Ismail AA, Kini G, Ibrahima IA, Koopmanb B. Synthesis of highly ordered cubic zeolite A and its ion-exchange behavior. *Colloid Surf A*. 2009;348:87–92.
50. Agrawal A, Sahu KK, Pandey BD. A comparative adsorption study of copper on various industrial solid wastes. *AIChE J*. 2004;50: 2430–2438.
51. Inglezakis VJ. Solubility-normalized Dubinin-Astakhov adsorption isotherm for ion-exchange systems. *Microporous Mesoporous Mater*. 2007;103:72–81.
52. El-Rahman KMA, El-Kamash AM, El-Sourougy MR, Abdel-Moniem NM. Thermodynamic modeling for the removal of Cs^{+}, Sr^{2+}, Ca^{2+} and Mg^{2+} ions from aqueous waste solutions using zeolite A. *J Radioanal Nucl Chem*. 2006;268:221–230.
53. Dron J, Dodi A. Comparison of adsorption equilibrium models for the study of Cl^{-}, NO_3^{-} and SO_4^{2-} removal from aqueous solutions by an anion exchange resin. *J Hazard Mater*. 2011;190:300–307.
54. Gedik K, Imamoglu I. Affinity of clinoptilolite-based zeolites towards removal of Cd from aqueous solutions. *Sep Sci Technol*. 2008;43:1191–1207.

55. Wood GO. Affinity coefficients of the Polanyi/Dubinin adsorption isotherm equations: a review with compilations and correlations. *Carbon*. 2001;39:343–356.
56. Dobruskin VK. Micropore volume filling. A condensation approximation approach as a foundation to the Dubinin-Astakhov equation. *Langmuir*. 1998;14:3840–3846.
57. Sun C, Li C, Wang C, Qu R, Niu Y, Geng H. Comparison studies of adsorption properties for Hg (II) and Au (III) on polystyrene-supported bis-8-oxyquinoline-terminated open-chain crown ether. *Chem Eng J*. 2012;200–202:291–299.
58. Yousef RI, El-Eswed B, Al-Muhtaseb AH. Adsorption characteristics of natural zeolites as solid adsorbents for phenol removal from aqueous solutions: kinetics, mechanism, and thermodynamics studies. *Chem Eng J*. 2011;171:1143–1149.
59. Panayotova MI. Kinetics and thermodynamics of copper ions removal from wastewater by use of zeolite. *Waste Manage*. 2001;21: 671–676.
60. Ho YS, Porter JF, McKay G. Equilibrium isotherm studies for the sorption of divalent metal ions onto peat: copper, nickel and lead single component systems. *Water Air Soil Pollut*. 2002;141:1–33.
61. Atar N, Olgun A, Wang S. Adsorption of cadmium (II) and zinc (II) on boron enrichment process waste in aqueous solutions: batch and fixed-bed system studies. *Chem Eng J*. 2012;192:1–7.
62. Pradas EG, Sánchez MV, Cruz FC, Viciana MS, Pérez MF. Adsorption of cadmium and zinc from aqueous solution on natural and activated bentonite. *J Chem Technol Biotechnol*. 1994;59:289–295.
63. Breck DW, Eversole WG, Milton RM, Reed TB, Thomas TL. Crystalline zeolites. I. the properties of a new synthetic zeolite, type A. *J Am Chem Soc*. 1956;78:5963–5972.
64. Allen HE, Cho SH, Neubecker TA. Ion exchange and hydrolysis of type A zeolite in natural waters. *Water Res*. 1983;17:1871–1879.

Manuscript received Dec. 15, 2013, and revision received Nov. 3, 2014.